2015 IEEE 54th Annual Conference on Decision and Control (CDC)
December 15-18, 2015. Osaka, Japan

Robust H_∞ Output-Feedback Control for Path Following of Autonomous Ground Vehicles

Hui Jing[1,2], Chuan Hu[3], Fengjun Yan[3], Mohammed Chadli[4], Rongrong Wang[1] and Nan Chen[1]

Abstract— **This paper presents a robust H_∞ output-feedback control strategy for the path following of autonomous ground vehicles (AGVs). Considering the vehicle lateral velocity is usually hard to measure with low cost sensors, a robust H_∞ static output-feedback controller based on a mixed genetic algorithms (GA)/linear matrix inequality (LMI) approach is proposed to realize the path following without the information of the lateral velocity. The proposed controller is robust to the external disturbances and the uncertainties of the vehicle/environment parameters/states, including the tire cornering stiffness, vehicle longitudinal velocity, yaw rate and road curvature. Simulation results based on the CarSim-Simulink joint platform using a high-fidelity and full-car model have verified the effectiveness of the proposed control approach.**

I. INTRODUCTION

Increasing demands and developing technologies on the mobility, efficiency, and safety motivate the development of intelligent transportation means. Autonomous ground vehicle (AGV), with the improved security and better road utilization, has become an emerging research focus [1], [2]. One of the most rudimentary issues for AGVs is path following [3] [4], whose control objective is to make the vehicle follow a predefined path with the path following errors (i.e., the lateral offset and the heading error) converged to zero.

The presences of the model uncertainties and external disturbances increase difficulties in path following control for AGVs, where model uncertainties may stem from the variations of the vehicle/environment parameters/states. Several control techniques were proposed to handle these problems, such as, PID control [5], sliding mode control (SMC) [6], model predictive control (MPC) [7], artificial neural network control [8], chained systems theory [9], and optimal control [10], etc. These literatures generally regarded that the vehicle lateral speed/sideslip angle can be measured. However, typically the vehicle lateral speed/sideslip angle can only be measured by expensive sensors, e.g., dual antenna GPS system or optical sensors. From the practical application perspective, the output-feedback control is a feasible alternative to be adopted in the path following control of AGVs to reduce the vehicle control cost.

Although numerous output-feedback techniques for vehicle handling and stability control were proposed in previous research works [12]–[14], literatures which applied output-feedback strategies in the path following control of AGVs were still relatively limited. [15] presented the design of a piecewise affine output-feedback controller for vehicle lane keeping based on bilinear matrix inequalities optimization procedure, which was solved using the V-K-method. In [16], vision-based control strategies were presented for decentralized stabilization of unmanned vehicle formations, and an output-feedback approach using a high-gain observer was proposed to estimate the derivative of vehicles' relative position. In [17], an output-feedback adaptive neural network (NN) control was presented for transportation vehicles, incorporating a linear dynamic compensator to achieve stable dynamic balance and tracking of the desired given trajectories. An observer-based fuzzy controller was proposed in [18], which integrated H_∞ control and optimal control strategies so that without knowing road's curvature, the vehicle can keep its lane on a curved highway.

Nevertheless, few literatures simultaneously dealt with the uncertainties of the vehicle/environment parameters/states and the external disturbances in the output-feedback path following control framework for AGVs. To this end, this paper proposes a robust H_∞ output-feedback path following controller for AGVs considering the external disturbances and model uncertainties. The proposed controller aims at making the vehicle track the desired path with the desired lateral and longitudinal velocities, with the active front-wheel steering (AFS) and the driving force. The main contributions of this paper lie on two aspects: 1) A robust H_∞ static output-feedback controller based on a mixed genetic algorithms (GA)/linear matrix inequality (LMI) technique is designed to regulate the controlled outputs without using the information of the vehicle lateral velocity; 2) The uncertainties of the tire cornering stiffness, the vehicle longitudinal velocity and yaw rate, and road curvature, as well as the external disturbances are simultaneously considered in the robust controller design.

The rests of the paper are organized as follows. The modeling of path following and vehicle lateral dynamic are presented in Section II. The robust static H_∞ output-feedback controller is proposed in Section III. Simulation based on a high-fidelity and full-vehicle model via CarSim-

[1,2]Hui Jing is with School of Mechanical Engineering, Southeast University, Nanjing 211189, P.R. China, and School of Mechanical and Electrical Engineering, Guilin University of Electronic Technology, Guilin 541004, P.R. China. jinghui@guet.edu.cn

[1]Rongrong Wang and Nan Chen are with School of Mechanical Engineering, Southeast University, Nanjing 211189, P.R. China. wrr06fy@gmail.com; nchen@seu.edu.cn

[3]Chuan Hu and Fengjun Yan are with the Department of Mechanical Engineering, McMaster University, Hamilton, ON L8S4L8, Canada. huc7@mcmaster.ca; yanfeng@mcmaster.ca

[4]Mohammed Chadli is with the University of Picardie Jules Verne, MIS (E.A. 4290). 80039, Amiens, France. mohammed.chadli@u-picardie.fr

This work was partly supported by National Natural Science Foundation of China (51375086, 51505081), Foundation of Education Office of Guangxi Province, China (KY2015YB101), and the Opening Project of Guangxi Colleges and Universities Key Laboratory of UAV Remote Sensing(WRJ2015KF02).

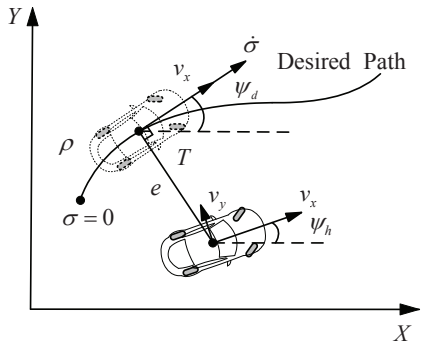

Fig. 1. Schematic diagram of path following model.

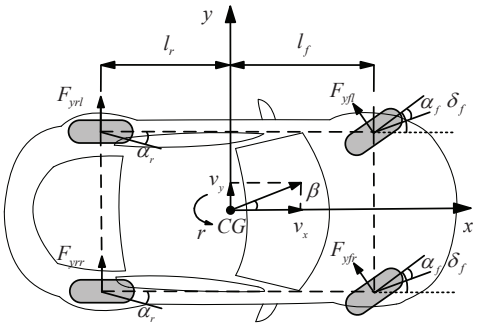

Fig. 2. Schematic diagram of a vehicle planar motion model.

Simulink platform is presented in Section IV, followed by the conclusion in Section V.

II. System Modelling And Problem Formulation

A. Path Following Model

The path following model is shown in Fig. 1, where e denotes the lateral offset from the vehicle center of gravity (CG) to the closest point T on the desired path. The heading error ψ is defined as the heading error between actual heading angle ψ_h and desired heading angle ψ_d, thus $\psi = \psi_h - \psi_d$, and $\dot{\psi}_h = r$, with r being the yaw rate of the vehicle. v_x and v_y is the longitudinal and lateral velocty of the vehicle, respectively. σ denotes the curvilinear coordinate (arc-length) of point T along the path from an initial position predetermined, while we know $\sigma \geq 0$, $\dot{\sigma} = d\sigma/dt$. Finally, $\rho(\sigma)$ represents the curvature of the desired path at the point T. The curvilinear coordinate of points T along the path σ can be given as

$$\dot{\sigma} = \frac{1}{1 - e \cdot \rho(\sigma)}(v_x \cos\psi - v_y \sin\psi). \tag{1}$$

Based on the Serret-Frenet equation [19], the path following dynamics of vehicle can be modeled as

$$\begin{cases} \dot{e}_1 = v_x \sin\psi + v_y \cos\psi \\ \dot{\psi} = r - \rho(\sigma) v_x \end{cases}, \tag{2}$$

where $e_1 = e$. With small heading angle error assumption, the above equation can be rewritten as

$$\begin{cases} \dot{e}_1 = v_x \psi + v_y + d_1 \\ \dot{\psi} = r - \rho(\sigma) v_x \end{cases}, \tag{3}$$

where d_1 represents the modeling error and external disturbance.

B. Vehicle Model

A schematic diagram of a vehicle model is shown in Fig. 2. Assuming the front-wheel steering angle is small, the vehicle's handling dynamics in the yaw plane can be expressed as

$$\begin{cases} \dot{v}_y = \frac{1}{m}(F_{yf} + F_{yr}) - v_x r + d_2 \\ \dot{r} = \frac{1}{I_z}(l_f F_{yf} - l_r F_{yr}) + d_3 \end{cases}, \tag{4}$$

where m and I_z is the mass and yaw inertia of the vehicle, respectively. d_2 and d_3 are external disturbances. The front and rear tire lateral forces F_{yf}, F_{yr} are functions of tire slip angles and can be modelled as,

$$F_{yf} = C_f \alpha_f, \quad F_{yr} = C_r \alpha_r, \tag{5}$$

where $C_{f,r}$ are the front and rear tire cornering stiffness values, $\alpha_{f,r}$ are the wheel slip angles which can be calculated as

$$\alpha_f = \delta_f - \frac{l_f r}{v_x} - \frac{v_y}{v_x}, \quad \alpha_r = \frac{l_r r}{v_x} - \frac{v_y}{v_x}, \tag{6}$$

where δ_f is the front wheel steering angle. It can be deduced that (4) can be rewritten as

$$\begin{cases} \dot{v}_y = a_{11} v_y + a_{12} r + b_1 \delta_f + d_2 \\ \dot{r} = a_{21} v_y + a_{22} r + b_2 \delta_f + d_3 \end{cases}, \tag{7}$$

where the model parameters in (7) are given as

$$\begin{aligned} &a_{11} = -\tfrac{(C_f + C_r)}{m v_x}, \quad a_{12} = -v_x - \tfrac{(l_f C_f - l_r C_r)}{m v_x}, \\ &a_{21} = \tfrac{(l_r C_r - l_f C_f)}{I_z v_x}, \quad a_{22} = -\tfrac{\left({l_f}^2 C_f + {l_r}^2 C_r\right)}{v_x I_z}, \\ &b_1 = \tfrac{C_f}{m}, \quad b_2 = \tfrac{l_f C_f}{I_z}. \end{aligned} \tag{8}$$

As $a_x = \dot{v}_x - r v_y$ and $a_x = F_X/m + d_4$, where d_4 is the unmodeled tire rolling resistance and wind drag, $F_X = \sum F_{xi}$ means the generalized longitudinal tire force with F_{xi} being the longitudinal force of the ith tire, we can get

$$\dot{v}_x = r v_y + F_X/m + d_4. \tag{9}$$

Define $e_2 = v_x - v_{xr}$ with v_{xr} being the desired longitudinal velocity, and $\dot{e}_2 = \dot{v}_x - \dot{v}_{xr}$, we have

$$\begin{cases} \dot{e}_2 = r v_y + F_X r/m - \dot{v}_{xr} + d_4 \\ \dot{\psi} = r - \rho(\sigma) v_x = r - \rho(\sigma) e_2 - \rho(\sigma) v_{xr} \end{cases}. \tag{10}$$

Combined (3) with (7) and (10), we can get

$$\begin{cases} \dot{\psi} = r - \rho(\sigma) e_2 - \rho(\sigma) v_{xr} \\ \dot{v}_y = a_{11} v_y + a_{12} r + b_1 \delta_f + d_2 \\ \dot{r} = a_{21} v_y + a_{22} r + b_2 \delta_f + d_3 \\ \dot{e}_1 = v_x \psi + v_y + d_1 \\ \dot{e}_2 = r v_y + F_X/m - \dot{v}_{xr} + d_4 \end{cases}. \tag{11}$$

Define the state vector $x(t) = [\psi,\ v_y,\ r,\ e_1,\ e_2]^T$, the control input $u(t) = [\delta_f, F_X]^T$, and the disturbance $w(t) =$

$[-\rho(\sigma)v_{xr},\ d_1,\ d_2,\ d_3,\ -\dot{v}_{xr}+d_4]^T$, the state-space form of the model can be given as

$$\dot{x}(t) = Ax(t) + Bu(t) + w(t). \tag{12}$$

where

$$A = \begin{bmatrix} 0 & 0 & 0 & 1 & -\rho \\ 0 & 0 & a_{11} & a_{12} & 0 \\ 0 & 0 & a_{21} & a_{22} & 0 \\ 0 & v_x & 1 & 0 & 0 \\ 0 & 0 & r & 0 & 0 \end{bmatrix}, B = \begin{bmatrix} 0 & 0 \\ b_1 & 0 \\ b_2 & 0 \\ 0 & 0 \\ 0 & \frac{1}{m} \end{bmatrix}.$$

Note that the vehicle front-wheel steering angle δ_f and heading error ψ are assumed to be small in the vehicle modelling, which is used to facilitate the controller design. Based on this assumption a robust controller will be designed to attenuate the effects of unmodelled dynamics and disturbance.

C. Vehicle Modelling with Parameter Uncertainties

The tire cornering stiffness is a time-varying and unknown parameter due to the change of road conditions and vehicle states, we represent the varying cornering stiffnesses as

$$\begin{aligned} C_f &= C_{0f} + \lambda_f \tilde{C}_f, \\ C_r &= C_{0r} + \lambda_r \tilde{C}_r, \end{aligned} \tag{13}$$

where $\lambda_{f,r}$ are time-varying parameters which satisfy $|\lambda_i| \leq 1, (i = f, r)$, C_{0f} and C_{0r} are the nominal values of C_f and C_r, respectively. So we have

$$\begin{aligned} A &= A_0 + \Delta A, \\ B &= B_0 + \Delta B, \end{aligned} \tag{14}$$

where A_0 and B_0 is the nominal values of matrices A and B, respectively. ΔA and ΔB are the variations of matrices A and B, respectively.

There are still time-varying parameters v_x , $1/v_x$, ρ and r in the system model matrices. Since the longitudinal speed v_x is usually bounded, we can assume that v_x varies in the range $[v_{x\min},\ v_{x\max}]$, and thus $1/v_x$ varies in the range of $[1/v_{x\max},\ 1/v_{x\min}]$. The same assumption can be applied on ρ and r, i.e., ρ is bounded in the range $[\rho_{\min},\ \rho_{\max}]$, and r is bounded in the range $[r_{\min},\ r_{\max}]$, respectively. In this study, a polytope which contains $2^4 = 16$ vertices is employed to cover all the possible choices for the parameter pair $[v_x,\ 1/v_x,\ \rho,\ r]$. The vertices' coordinates can be rewritten as $\hat{\vartheta}_1 = v_{x\min},\ \hat{\vartheta}_2 = v_{x\max},\ \tilde{\vartheta}_1 = 1/v_{x\min},\ \tilde{\vartheta}_2 = 1/v_{x\max}, \bar{\vartheta}_1 = \rho_{\min},\ \bar{\vartheta}_2 = \rho_{\max},\ \check{\vartheta}_1 = r_{\min},\ \check{\vartheta}_2 = r_{\max}$.

Then the varying parameters v_x, $1/v_x$, ρ and r can be represented by a summation of the vertices' coordinates as

$$\begin{aligned} v_x &= \sum_{i=1}^{2} \hat{h}_i(t)\hat{\vartheta}_i, \quad \frac{1}{v_x} = \sum_{i=1}^{2} \tilde{h}_i(t)\tilde{\vartheta}_i, \\ \rho &= \sum_{i=1}^{2} \bar{h}_i(t)\bar{\vartheta}_i, \qquad r = \sum_{i=1}^{2} \check{h}_i(t)\check{\vartheta}_i, \end{aligned} \tag{15}$$

with the weighting factors as

$$\begin{aligned} \hat{h}_1(t) &= \frac{v_{x\max} - v_x}{v_{x\max} - v_{x\min}}, & \hat{h}_2(t) &= \frac{v_x - v_{x\min}}{v_{x\max} - v_{x\min}}, \\ \tilde{h}_1(t) &= \frac{1/v_{x\max} - 1/v_x}{1/v_{x\max} - 1/v_{x\min}}, & \tilde{h}_2(t) &= \frac{1/v_x - 1/v_{x\min}}{1/v_{x\max} - 1/v_{x\min}}, \\ \bar{h}_1(t) &= \frac{\rho_{\max} - \rho}{\rho_{\max} - \rho_{\min}}, & \bar{h}_2(t) &= \frac{\rho - \rho_{\min}}{\rho_{\max} - \rho_{\min}}, \\ \check{h}_1(t) &= \frac{r_{\max} - r}{r_{\max} - r_{\min}}, & \check{h}_2(t) &= \frac{r - r_{\min}}{r_{\max} - r_{\min}}. \end{aligned}$$

Define

$$h_1 = \acute{h}_{1111}, h_2 = \acute{h}_{1112},\ ...,\ h_{16} = \acute{h}_{2222},$$

with

$$\acute{h}_{mnij} = \hat{h}_m \tilde{h}_n \bar{h}_i \check{h}_j,\ (m = 1, 2, n = 1, 2, i = 1, 2, j = 1, 2).$$

The system plant (12) can be rewritten in the polytopic form as

$$\begin{aligned} \dot{x}(t) &= \sum_{i=1}^{16} h_i(t)[A_i x(t) + Bu(t) + w(t)] \\ &= \sum_{i=1}^{16} h_i(t)\big[(A_{0i} + \Delta A_i)x(t) \\ &\qquad + (B_0 + \Delta B)u(t) + w(t)\big], \end{aligned} \tag{16}$$

where the matrices A_{0i} and ΔA_i can be obtained by replacing v_x, $1/v_x$, ρ, and r with $\hat{\vartheta}_i$, $\tilde{\vartheta}_i$, $\bar{\vartheta}_i$ and $\check{\vartheta}_i$ in A_0 and ΔA, respectively. Note that based on the h_i definition, we have

$$\sum_{i=1}^{16} h_i(t) = 1, \quad h_i(t) \geq 0. \tag{17}$$

Based on the definitions of ΔA_i and ΔB, we have

$$[\Delta A_i \quad \Delta B] = H\Lambda_1[E_{1i} \quad E_2], \tag{18}$$

where

$$\begin{aligned} H &= \begin{bmatrix} 0 & 1 & 0 & 0 & 0 \\ 0 & 0 & 1 & 0 & 0 \end{bmatrix}^T,\ \Lambda_1 = diag\{\lambda_f, \lambda_f\}, \\ E_{1i} &= \begin{bmatrix} 0 & -\frac{(\tilde{C}_f + \tilde{C}_r)\tilde{\vartheta}_i}{m} & -\frac{(\tilde{C}_f l_f - \tilde{C}_r l_r)\tilde{\vartheta}_i}{m} & 0 & 0 \\ 0 & \frac{(\tilde{C}_r l_r - \tilde{C}_f l_f)\tilde{\vartheta}_i}{I_z} & -\frac{(\tilde{C}_f l_f^2 + \tilde{C}_r l_r^2)\tilde{\vartheta}_i}{I_z} & 0 & 0 \end{bmatrix}, \\ E_2 &= \begin{bmatrix} \frac{\tilde{C}_f}{m} & 0 \\ \frac{\tilde{C}_f l_f}{I_z} & 0 \end{bmatrix}. \end{aligned}$$

Note that the assumption $\lambda_f = \lambda_r$ is used in the system modelling. Since the road conditions are usually uniform to the front and rear wheels, it is reasonable to assume that $\lambda_f = \lambda_r$. The possible computational burden and design conservation can be avoided since the number of the uncertainty parameters in matrices ΔA_i and ΔB has been reduced owing to this assumption.

D. Problem Statement

As for the state feedback controller design, all the elements in the state vector $x(t) = [e_1,\ \psi,\ v_y,\ r,\ e_2]^T$ should be measured. The vehicle lateral offset e_1, heading error ψ and vehicle longitudinal velocity error e_2 can be measured by

cheaper equipments such as ordinary GPS. Vehicle yaw rate r can be measured with vehicle on-board sensors such as gyroscope, or it can be synthesized from accelerometers. However, the vehicle lateral speed is usually hard to measure by cheap seasors. Therefore, the state-feedback based control schemes is difficult to applied on commercial vehicles. Consequently, the output-feedback based control schemes should be considered in real application. For the output-feedback controller, only the vehicle lateral offset e_1, heading error ψ, vehicle yaw rate r and vehicle longitudinal velocity error e_2 are taken as the measured outputs in this study. The measured output vector $y(t) = [e_1,\ \psi,\ r,\ e_2]^T$ is defined as

$$y(t) = C_1 x(t). \tag{19}$$

In order to the improve path following performance of the vehicle, e_1, ψ and e_2 should be as small as possible. Simultaneously, to enhance the handling stability, the vehicle lateral speed v_y should not be large. Therefore the controlled output vector $z(t) = [e_1,\ \psi,\ v_y,\ e_2]^T$ is defined as

$$z(t) = C_2 x(t). \tag{20}$$

The path following vehicle model can be rewritten as

$$\begin{cases} \dot{x}(t) = \sum_{i=1}^{16} h_i(t)\big[(A_{0i} + \Delta A_i)x(t) \\ \qquad\qquad + (B_0 + \Delta B)u(t) + w(t)\big]. \\ y(t) = C_1 x(t) \\ z(t) = C_2 x(t) \end{cases} \tag{21}$$

The control objective is to design a robust output-feedback controller to generate a control signal $u(t)$, such that the closed-loop system in (21) is asymptotically stable and has the following H_∞ disturbance attenuation performance in the presence of model uncertainties and external disturbance

$$\int_0^t z^T(t)z(t)dt \le \gamma^2 \int_0^t w^T(t)w(t)dt, \tag{22}$$

where γ is the prescribed attenuation level.

III. Robust Output-Feedback Controller Design

A. Static output-feedback controller design

We propose the design of the following output-feedback controller as

$$u(t) = \sum_{i=1}^{16} h_i(t)K_i y(t) = \sum_{i=1}^{16} h_i(t)K_i C_1 x(t), \tag{23}$$

where K_i is the control gains to be designed. Substituting (23) into (21), the closed-loop system can be written as,

$$\begin{cases} \dot{x}(t) = \sum_{i=1}^{16} h_i(t)\big[\tilde{A}_i x(t) + w(t)\big] \\ z(t) = \tilde{C}x(t) \end{cases}, \tag{24}$$

where $\tilde{A}_i = \bar{A}_i + H\Lambda_1\bar{E}_i$, $\bar{A}_i = A_{0i} + B_0K_iC_1$, $\bar{E}_i = E_{1i} + E_2K_iC_1$, and $\tilde{C} = C_2$.

In order to deal with the parameter/state uncertainties, we introduce the following lemmas:

Lemma 1 [20]: Given a positive scalar γ, the closed-loop system in (24) is asymptotically stable and satisfies the H_∞ performance index (22), if and only if there exists a symmetric positive definite matrix P satisfying the following condition

$$\begin{bmatrix} \mathrm{sys}\{\tilde{A}^T P\} & P & \tilde{C}^T \\ * & -\gamma^2 I & 0 \\ * & * & -I \end{bmatrix} < 0, \tag{25}$$

where here and everywhere in the sequel, $\mathrm{sys}\{\bullet\}$ denotes $\bullet + \bullet^T$, $*$ denotes the symmetric elements in a symmetric matrix.

Lemma 2 [11]: Let $Y = Y^T$, Γ and Ψ be the real matrices with proper dimensions, and $\tilde{N}$ satisfies $\Lambda^T\Lambda < I$, then the following condition

$$Y + \Gamma\Lambda\Psi + \Psi^T\Lambda^T\Gamma^T < 0, \tag{26}$$

holds if and only if there exists a positive scalar $\varepsilon > 0$ such that

$$Y + \epsilon\Gamma\Gamma^T + \epsilon^{-1}\Psi^T\Psi < 0. \tag{27}$$

Now we are in the position to propose the robust static output-feedback controller design method.

Theorem 1: Given a positive constant γ, the closed-loop system in (24) is asymptotically stable with $w(t) = 0$, and can satisfy the H_∞ performance index (22) for all $w(t) \in [0, \infty)$, if there exists a symmetric positive definite matrix Q and scalar $\varepsilon_i > 0$ such that

$$\begin{bmatrix} \Xi_i & I & QC_2^T & \varepsilon_i H & Q\tilde{E}_i^T \\ * & -\gamma^2 I & 0 & 0 & 0 \\ * & * & -I & 0 & 0 \\ * & * & * & -\varepsilon_i I & 0 \\ * & * & * & * & -\varepsilon_i I \end{bmatrix} < 0, \tag{28}$$

where $\Xi_i = \mathrm{sys}\{A_{0i}Q + B_0K_iC_1Q\}$.

Proof: Since $\tilde{A}_i = \bar{A}_i + H\Lambda_1\bar{E}_i$ with $\bar{A}_i = A_{0i} + B_0K_iC_1$ and $\bar{E}_i = E_{1i} + E_2K_iC_1$, we have

$$\begin{aligned} \mathrm{sys}\{\tilde{A}_i^T P\} &= \mathrm{sys}\{(\bar{A}_i + H\Lambda_1\bar{E}_i)^T P\} \\ &= \mathrm{sys}\{\bar{A}_i^T P\} + \mathrm{sys}\{PH\Lambda_1\bar{E}_i\}. \end{aligned} \tag{29}$$

Then the left side of (25) can be rewritten as:

$$\begin{aligned} &\begin{bmatrix} \mathrm{sys}\{\tilde{A}^T P\} & P & \tilde{C}^T \\ * & -\gamma^2 I & 0 \\ * & * & -I \end{bmatrix} \\ &= \begin{bmatrix} \mathrm{sys}\{\bar{A}^T P\} & P & \tilde{C}^T \\ * & -\gamma^2 I & 0 \\ * & * & -I \end{bmatrix} \\ &\quad + \mathrm{sys}\left\{ \begin{bmatrix} PH \\ 0 \\ 0 \end{bmatrix} \Lambda_1 \begin{bmatrix} \bar{E}_i & 0 & 0 \end{bmatrix} \right\}. \end{aligned} \tag{30}$$

It follows form *Lemma* 2 that the following inequality holds

$$\begin{bmatrix} \bar{\Xi}_i & P & C_2^T & \varepsilon_i PH & P\tilde{E}_i^T \\ * & -\gamma^2 I & 0 & 0 & 0 \\ * & * & -I & 0 & 0 \\ * & * & * & -\varepsilon_i I & 0 \\ * & * & * & * & -\varepsilon_i I \end{bmatrix} < 0, \qquad (31)$$

with $\bar{\Xi}_i = \text{sys}\{P\bar{A}_{0i}^T + PB_0K_iC_1\}$. Define $Q = P^{-1}$, and perform a congruence transformation with $\Gamma = \text{diag}\{Q,\ I,\ I,\ I,\ I\}$ to the above inequality, the inequality (28) holds. This completes the proof of the *Theorem* 1.

Note that there are still nonlinear terms in (28), i.e., the terms Q and K_i are coupled in Ξ_i, and these nonlinear terms cannot be removed by the change of variable which is usually used in the robust H_∞ state-feedback controllers. In addition, generally there is no analytical solution to the above static output-feedback problem subjected to polytopic uncertainties. Inspired by the application of the GA in static output-feedback controller design [21], this paper adopts the GA and Matlab LMI toolbox to obtain the optimal static output-feedback gains.

B. Mixed GA/LMI algorithm

GA, as an evolutionary computation algorithm, has been widely used in the control applications since it does not require extensive calculations for optimization problems [22] [23]. This algorithm calculates the objective function value by using the concepts of chromosomes and genetic operators to find the best generations until the termination condition is satisfied. The robust static output-feedback controller is designed via mixed GA/LMI algorithm through searching the optimal gains K_i, which can be briefly outlined as following

Minimize γ, subject to :

(1) Equation (28)

(2) the eigenvalue of $\tilde{A}_i$ in closed loop is negative, i.e. $\text{Re}(\lambda(\tilde{A}_i)) < 0$

(3) the eigenvalue of $\tilde{A}$ in closed loop is negative, i.e. $\text{Re}(\lambda(\tilde{A})) < 0$

where $\lambda(\bullet)$ denotes the eigenvalue of $(\bullet)$, $\text{Re}(\bullet)$ denotes the real part of $(\bullet)$. The main steps of of mixed GA/LMI are shown as follows:

Step 1: Initialize the GA parameters, i.e. initial population size, selection factor, crossover factor, mutation factor and termination conditions;

Step 2: Initialize K_i as the first generation (note that the initial value of K_i can be selected randomly or manually);

Step 3: Solve the inequality (28) in the *Theorem 1*;

Step 4: If $\text{Re}(\lambda(\tilde{\text{A}}_\text{i})) < 0$, $\text{Re}(\lambda(\tilde{A})) < 0$, and the inequality (28) are simultaneously satisfied, then go to *Step 5*. Otherwise, go to *Step 2* to regenerate the output-feedback gains K_i (note that the regeneration of K_i can be performed by Matlab toolbox, i.e. selection, crossover and mutation operations);

Step 5: Minimize γ with matlab LMI toolbox. If γ is smaller than γ^* which is predefined in the *Step 1* , then we have $\gamma^* = \gamma$, and go to *Step 2* to regenerate the output feedback gains K_i. Otherwise, with γ^* no changes and the algorithm directly go to *Step 2* to regenerate the output-feedback gains K_i. Here, the γ^* is a predefined positive scalar which is sufficiently small;

Step 6: If the decrease of γ^* does not exceed a given small value, the algorithm terminates. Otherwise, go to *Step 2* to regenerate the output-feedback gains K_i.

IV. Simulation Studies

In this section, simulation based on a high-fidelity and full-vehicle model constructed in CarSim is conducted to verify the effectiveness and advantage of the proposed control method. The vehicle parameters are listed as: $m = 1500$ kg, $I_z = 2000$ kg·m^2, $l_s = 0.8$ m, $l_f = 1.3$ m, $l_r = 1.4$ m, $C_f = C_r = 40000$ N/rad with $\pm 20\%$ uncertainty, respectively, $v_{x\,\min} = 18$ m/s, $v_{x\,\max} = 30$ m/s, $\rho_{\min} = -0.05$ m^{-1}, $\rho_{\max} = 0.05$ m^{-1}, $r_{\min} = -0.4$ rad/s, and $r_{\max} = 0.4$ rad/s.

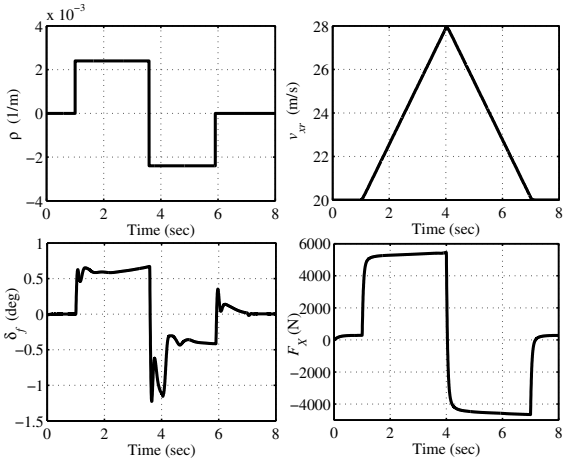

Fig. 3. The simulation results for the road curvature, desired longitudinal velocity, and control inputs.

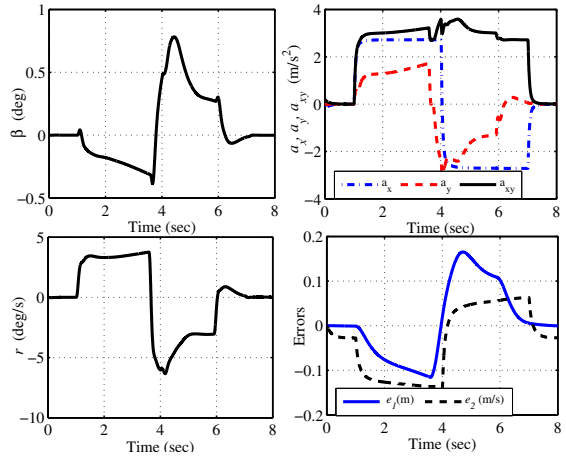

Fig. 4. The simulation results for the sideslip angle, vehicle acceleration, yaw rate, and tracking errors.

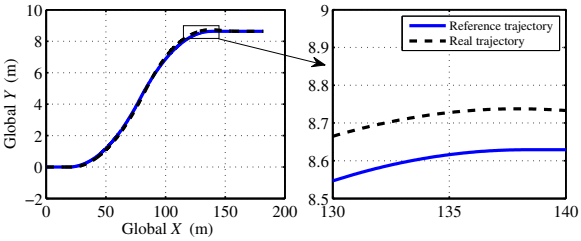

Fig. 5. Global trajectory of the vehicle.

The simulation, which is similar to lane-change maneuver, is executed on a low adherence road ($\mu = 0.4$). The simulation results for the road curvature, desired longitudinal velocity, and control inputs are presented in Fig. 3. The sub-figure for the curvature is to form a lane-change path. To validate the proposed approach, we suppose that the road curvature includes a sudden change. Even under such conditions, the steering angle is still small and maintained in the reasonable region. One can also see from Fig. 3 that when the road curvature and reference vehicle velocity vary, the front wheel steering angle and the generalized longitudinal tire force are maintained in reasonable regions. By using the proposed controller the vehicle shows high performance in the trajectory tracking and velocity tracking, as shown in Fig. 4 and Fig. 5, respectively. Simultaneously, even on the low-adherence road surface, the vehicle states such as vehicle sideslip angle, yaw rate, and accelerations shown in Fig. 4 can still be well controlled, respectively. Note that a low-adherence road ($\mu = 0.4$) is used and the combined vehicle lateral acceleration $a_{xy} = \sqrt{a_x^2 + a_y^2}$ of the controlled vehicle is very close to $0.4g$, which means that the vehicle reaches the friction limit, which further proves the effectiveness of the proposed controller.

V. Conclusion

A robust output-feedback control strategy is designed to improve path following performance and vehicle stability of an AGV. Considering the high cost of current available sensors for vehicle lateral velocity measurement, a robust H_∞ static output-feedback controller is designed to control the vehicle path following without using the lateral velocity information. As nonlinear terms cannot be removed by the change of variables, a mixed GA/LMI approach is proposed to obtain the proper static output-feedback gains. Both external disturbances and parameter/state uncertainties are considered in the controller design. Simulation results based on CarSim platform verify the effectiveness of the control approach.

References

[1] A. Broggi, P. Medici, P. Zani, A. Coati, and M. Panciroli, "Autonomous vehicles control in the VisLab intercontinental autonomous challenge," *Annu. Rev. Control*, vol. 36, no. 1, pp. 161-171, Apr. 2012.

[2] J. Levinson, J. Askeland, J. Becker, J. Dolson, D. Held, S. Kammel, and S. Thrun, "Towards fully autonomous driving: Systems and algorithms," in *Proc.IEEE Intell. Veh. Symp.*, pp. 163-168, 2011.

[3] V. Girbes, L. Armesto, and J. Tornero, "Path following hybrid control for vehicle stability applied to industrial forklifts," *Robot. Auton. Syst.* , vol. 62, no. 6, pp. 910-922, Jun. 2014.

[4] M. A. Zakaria, H. Zamzuri, R. Mamat, and S. A. Mazlan, "A path tracking algorithm using future prediction control with spike detection for an autonomous vehicle robot," *Int. J. Adv. Robot. Syst.*, vol. 10, pp. 309-317, Aug. 2013.

[5] P. Zhao, J. Chen, T. Mei, and H. Liang, "Dynamic motion planning for autonomous vehicle in unknown environments," in *Proc.IEEE Intell. Veh. Symp.*, pp.284-289, 2011.

[6] H. Fang, L. Dou, J. Chen, R. Lenain, B. Thuilot, and P. Martinet, "Robust anti-sliding control of autonomous vehicles in presence of lateral disturbances," *Control Eng. Pract.*, vol. 19, no. 5, pp. 468-478, May. 2011.

[7] R. Lenain, B. Thuilot, C. Cariou, and P. Martinet, "High accuracy path tracking for vehicles in presence of sliding: Application to farm vehicle automatic guidance for agricultural tasks," *Auton. Robot.*, vol. 21, no. 1, pp. 79-97, Jun. 2006.

[8] W. Tsui, M. S. Masmoudi, F. Karray, I. Song, and M. Masmoudi, "Soft-computing-based embedded design of an intelligent wall/lane-following vehicle," *IEEE-ASME Trans. Mechatron.*, vol. 13, no. 1, pp. 125-135, Feb. 2008.

[9] U. Nunes and L. C. Bento, "Data fusion and path-following controllers comparison for autonomous vehicles," *Nonlinear Dyn.*, vol. 49, no. 4, pp. 445-462, Sep. 2007.

[10] A. Goodarzi, A. Sabooteh, and E. Esmailzadeh, "Automatic path control based on integrated steering and external yaw-moment control," *Proc. Inst. Mech Eng Pt K-J Multi-Body Dyn.*, vol. 222, no. 2, pp. 189-200, Jun. 2008.

[11] H. Du, N. Zhang, and F. Naghdy, "Velocity-dependent robust control for improving vehicle lateral dynamics," *Transport Res. C-Emer.*, vol. 19, pp. 454-468, Jun. 2011.

[12] S. Aouaouda, M. Chadli, and H. R. Karimi, "Robust static output-feedback controller design against sensor failure for vehicle dynamics," *IET Control Theory A.*, vol. 8, no. 9, pp. 728-737, Jun. 2014.

[13] H. Zhang, R. Wang, J. Wang, and Y. Shi, "Robust finite frequency H_∞ static-output-feedback control with application to vibration active control of structural systems," *Mechatronics*, vol. 24, Issue 4, pp. 354-366, Jun. 2014.

[14] R. E. Benton Jr. and D. Smith, "A static-output-feedback design procedure for robust emergency lateral control of a highway vehicle," *IEEE Trans. Control Syst. Technol.*, vol. 13, no. 4, pp. 618-623, Jul. 2005.

[15] A. Benine-Neto and S. Mammar, "Piecewise affine output feedback controller for vehicle lane keeping," in *American Control Conference (ACC)*, pp. 6533-6538, Jun. 2012.

[16] O. A. A. Orqueda, X. T.Zhang, and R. Fierro, "An output feedback nonlinear decentralized controller for unmanned vehicle coordination," *Int. J. Robust. Nonlin.*, vol. 17, pp. 1106-1128, Aug. 2007.

[17] Z. Li and C. Yang, "Neural-adaptive output control of a class of transportation vehicles based on wheeled inverted pendulum models," *IEEE Trans. Control Syst. Technol.*, vol. 20, no. 6, pp. 1583-1591, Nov. 2012.

[18] C. S. Ting, "An output-feedback fuzzy approach to guaranteed cost control of vehicle lateral motion," *Mechatronics*, vol. 19, no. 3, pp. 304-312, Apr. 2009.

[19] R. Skjetne and T. I. Fossen, "Nonlinear maneuvering and control of ships," in *Proc. MTS/IEEE Oceans, Honolulu, HI*, pp. 1808-1815, 2001.

[20] R. Wang, H. Zhang, and J. Wang, "Linear parameter-varying controller design for four wheel independently-actuated electric ground vehicles with active steering systems," *IEEE Trans. Control Syst. Technol.*, vol. 22, Issue 4, pp. 1281-1296, Jul. 2014.

[21] H. Y. Chung and S. M. Wu, "Hybrid approaches for regional Takagi-Sugeno static output feedback fuzzy controller design," *Expert Syst. Appl.*, vol. 36, Issue 2, pp. 1720-1730, Mar. 2009.

[22] N. Nimpitiwan and S. Kaitwanidvilai, "Static output feedback robust loop shaping control for grid connected inverter using genetic algorithms," *Int.J.Innov. Comput. I.*, vol. 8, no. 9, pp. 6081-6093, Sep. 2012.

[23] M. S. Fallah, R. B. Bhat, and W. F. Xie, "Optimized control of semiactive suspension systems using H_∞ robust control theory and current signal estimation," *IEEE-ASME Trans. Mechatron.*, vol. 17, no. 4, pp. 767-778, Aug. 2012.